IEEE Access
Multidisciplinary | Rapid Review | Open Access Journal

Received November 15, 2019, accepted November 27, 2019, date of publication December 4, 2019,
date of current version December 23, 2019.

Digital Object Identifier 10.1109/ACCESS.2019.2957668

SEMG-Based Human In-Hand Motion Recognition Using Nonlinear Time Series Analysis and Random Forest

YAXU XUE[1], XIAOFEI JI[2], DALIN ZHOU[3], JING LI[4], AND ZHAOJIE JU[3], (Senior Member, IEEE)

[1]School of Electrical and Mechanical Engineering, Pingdingshan University, Pingdingshan 467000, China
[2]School of Automation, Shenyang Aerospace University, Shenyang 110136, China
[3]School of Computing, University of Portsmouth, Portsmouth PO1 3HE, U.K.
[4]School of Information Engineering, Nanchang University, Nanchang 330000, China

Corresponding author: Zhaojie Ju (zhaojie.ju@port.ac.uk)

This work was supported in part by the High-level Talent Start-up Foundation of Pingdingshan University under Grant PXY-BSQD-2019011, in part by the DREAM project of EU FP7-ICT under Grant 611391, and in part by the Natural Science Foundation of China under Grant 51575412, Grant 51575338, and Grant 51575407.

ABSTRACT As a novel and non-invasive sensing technology, surface electromyography (SEMG) can record the bioelectrical signals on the skin surface quickly and effectively, and thus has been widely used in human motion assessment in fields like medical rehabilitation and human-computer interaction. In this paper, an SEMG-based in-hand motion recognition system is proposed to recognize ten kinds of popular hand motions. According to the human common movements in performing in-hand object manipulations, ten sets of in-hand motions, including translation, transfer, and rotation, are designed, and then a nonlinear time series analysis method of SEMG signal processing is proposed to better capture the nonlinearity of these motions. The detailed analysis method of the nonlinear data is presented, and the experimental results, including human in-hand motion recognition result, motion recognition results of different subjects, and comparison results of different algorithms performance, are analyzed and discussed in detail. Experimental results illustrate that the human in-hand motion recognition system proposed in this paper can effectively recognize these different in-hand movements with a better performance than other popular methods.

INDEX TERMS Empirical mode decomposition, maximal Lyapunov exponent, random forest, surface electromyography.

I. INTRODUCTION

With the advance of sensor technology and signal processing technology, surface electromyography (SEMG), as a novel sensing technology, has been widely used in the fields of multi-functional prosthetic hand control, clinical medicine and human-computer interaction [1]. SEMG collects the bioelectrical signals of superficial muscle and nerve trunk activity on the skin surface through electrodes and realizes the evaluation and simulation of muscle function through recording, filtering, amplifying, transmitting, and feeding back the collected bioelectrical signals. Since the SEMG signals of human hand motions while handling objects are weak and easily interfered by noise, electromagnetism, *etc.*, it is difficult to measure the SEMG signals. How to successfully collect signals, extract features, and classify different hand motions has become the key issue to realizing complex human hand motion recognition.

While performing different operating tasks, human can select appropriate grasping strategies and applied forces according to the characteristics of objects (shape, size, weight, *etc.*). Realizing hand dexterous manipulation is a complex process, involving electromyography information. Hence, it is important to choose a good and effective SEMG signal acquisition device. Most of the commonly used SEMG signal acquisition devices, such as FlexComp Infiniti System (manufactured by Thought Technology in Canada), MyoScan-Pro EMG Sensor (manufactured by Biometrics) and Motion Lab electromyograph (manufactured by Moiton-Labs in America), use wire transmission to store the collected

The associate editor coordinating the review of this manuscript and approving it for publication was Habib Ullah.

SEMG signals into data acquisition cards or specific medical apparatus for analysis and processing; the electrodes are attached to the surface of the target muscle, and mains supply is used as the electrode power supply [2]–[4]. Therefore, during SEMG signal collection, these data acquisition devices are inevitably faced with issues like electrode shift, power frequency interference, and electromagnetic interference.

The manipulation of objects by hand is accomplished by the coordination between fingers and palms. Multi-channel SEMG signal acquisition can ensure the information complexity of the myoelectric activity during hand motions [5]. Currently, the features used to represent the original SEMG signals mainly include time-domain features (mean value, variance, impulse factor, *etc.*), frequency-domain features (mean square frequency, frequency variance, *etc.*) and time-frequency domain features (wavelet coefficient, Hibert spectrum, marginal spectrum, *etc.*). Increasing efforts have been made in analysing the SEMG signals by using different features. Xue *et al.* used six typical time-domain features to extract multimodal perception signals, and realized the recognition of ten kinds of hand motions by ADAG algorithm, with an average recognition rate of 94.57% [6]. Wang *et al.* extracted the frequency-domain features of acceleration signals and recognized ten gestures through probability neural network with a recognition rate of 98.75% [7]. According to the six features of three feature types, Chen *et al.* recognized eight common rehabilitation training gestures through Back Propagation (BP) neural network, among which DAMV+IAV+AR feature combination achieved the highest recognition rate 97.71% [8]. In addition to the literature mentioned above, a large number of related scientific papers as well as technical demonstrations have already appeared in various robot journals and conferences.

To recognize the common hand motions accurately, various classical classifiers such as Neural Network [9]–[11], Support Vector Machine [12]–[14], and Hidden Markov Model [15]–[17] have been used to process SEMG signals. The experimental results show that these classifiers can achieve relatively high accuracy in motion classification, but may increase the time and space complexity of training and testing owing to complex structures. Moreover, they mainly focus on the categorization of actions caused by a single muscle contraction in the absence of objects, yet fail to consider the recognition of hand motions involving multiple muscle contractions as well as the uncertainties of SEMG signal resulted from muscle fatigue and different subjects.

Biomedical signals which are generated by complex self-regulating physiological systems show highly irregular fluctuations. As SEMG signals are highly nonlinear and non-stationary, it is necessary to use nonlinear dynamic method to represent SEMG signals. Empirical Mode Decomposition (EMD) is a new adaptive signal time-frequency processing method, which is especially suitable for the analysis and processing of nonlinear non-stationary signals [18]. Lyapunov Exponent (LE) analysis is capable of describing the nonlinear characteristics of non-stationary signals and is widely applied in the signal detection of chaotic systems, such as electroencephalogram signals, SEMG signals and arc voltage signals [19]. It has been confirmed in references [20] and [21] that LE analysis is able to detect SEMG changes caused by uncertain factors like muscle fatigue. Random forest (RF), as a nonlinear classifier characterized by simple model structure, few parameters, and fast training speed, can achieve good results in regression and classification of nonlinear SEMG data sets. There are few researchers to analyze the human hand motions by using the integration of nonlinear time analysis and random forest. Based on that, this paper studies the nonlinear time series analysis method of SEMG signal processing and classification using EMD+MLE+RF. The advantage of using EMD+MLE is that it can separate noise from effective signal and extract key eigenvectors from initial Lyapunov exponents. The recognition performance of the proposed SEMG-based in-hand motion recognition system is also compared with other popular classifiers via simulations. The rest of this paper is arranged as follows: Section II firstly introduces the proposed human hand motion recognition system and then illustrates the adopted theoretical method from data acquisition, signal preprocessing, feature extraction and motion recognition; Section III presents the detailed analysis of the experimental data; in Section IV, the experimental results, including total human hand motion recognition result, motion recognition results of different subjects, and comparison results of different algorithms performance, are analyzed and discussed in detail; the proposed method and direction of future study are summarized in Section V.

II. METHODS

A. IN-HAND MOTION RECOGNITION SYSTEM

Compared with simple gestures, Complex motions generally include three main features: 1) multifingered movements with or without the palm; 2) wrist movements cooperating closely with in-hand manipulation; and 3) changes in the hand's location and posture. To better recognize complex human in-hand movements, this paper proposes an SEMG-based in-hand motion recognition system for prosthetic hand control, as shown in Fig.1. The system contains five parts, namely, human upper limb determination, data acquisition, data preprocessing, feature extraction, and recognition algorithm.

First, ten self-defined signals of complex in-hand movements were collected by using an SEMG acquisition device; second, the original SEMG signals collected were preprocessed for feature extraction; finally, the extracted features were classified into different motion types through recognition algorithm and the recognition performance was verified.

1) Human upper limb determination: given that the grasping points, the number of fingers used, and operation habits would vary according to the operation tasks, thus, to improve the universality of the experimental results, the right hands of the subjects were used as the test hands in this paper. To ensure the effectiveness

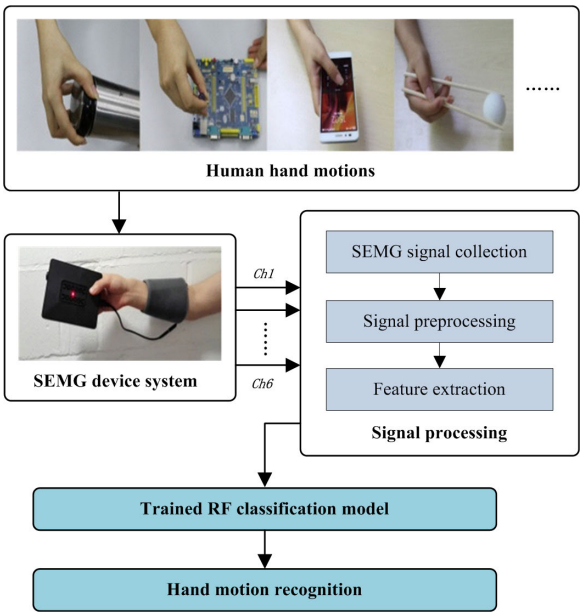

FIGURE 1. The framework of human hand motion recognition system.

of signal acquisition, the subjects' test hands had no neurological history.

2) Data acquisition and processing: the signals of ten typical human hand motions were collected by using SEMG acquisition device; the collected original signals were de-noised by using EMD algorithm and then the features of the signals were extracted by using MLE algorithm, through which the feature sets for hand movement classification were obtained.
3) Motion recognition: random forest algorithm was used to classify the feature sets and compared with other machine learning algorithms so as to verify its performance.

B. DATA COLLECTION

Based on some common hand gestures, ten kinds of in-hand movements, including transfer, translation and rotation, were designed in this paper, as shown in Fig.2. The SEMG of five forearm muscles, namely, flexor carpi radialis, flexor carpi ulnaris, flexor pollicis longus, flexor digitorum profundus, and extensor digitorum, were measured. To obtain clearer signals, subjects were scrubbed with alcohol and shaved if necessary and then electrodes were applied over the body using electrode sleeve. Electrodes locations were selected according to the musculoskeletal of these five muscles and confirmed by muscle specific contractions, which include manually resisted finger flexion, extension, and abduction. Ten healthy subjects were selected for data collection, including 8 males and 2 females, with an average age of 25 $\pm$ 3.6 year's old, average height of 168 $\pm$ 13 cm, and average weight of 63 $\pm$ 15.4 kg. All participants gave informed consent prior to the experiments.

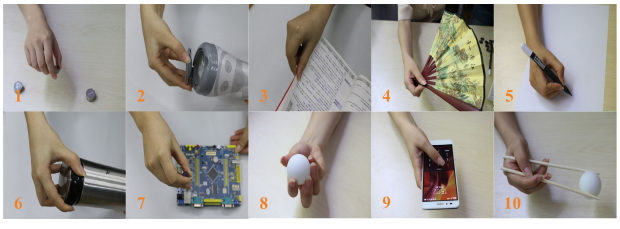

FIGURE 2. Ten self-defined in-hand motions.

The detailed presentation of ten in-hand motions is listed in Table 1. In view of the fact that the operation habits of different subjects vary even for the same object, such as grasping points and the number of fingers used, all the subjects had undergone strict operation training before the experiment. Every motion lasted for about 3 seconds to record SEMG and the duration of each run of the experiment was about 20 seconds. Each subject performed each action ten times and was given a two-minute break after completing one to ensure that the signal collection was not interfered by muscle fatigue.

TABLE 1. Presentation of ten in-hand motions.

Hand motion	Description
Motion 1	Transfer coins from one place to another
Motion 2	Open a box using five fingers
Motion 3	Continuous turning pages in a book
Motion 4	Open a fan with one hand
Motion 5	Pick up a pen to position it for write
Motion 6	Twist open a lid on a big water cup using five fingers
Motion 7	Screw off the screw on the circuit board
Motion 8	Grasp a ping-pong using five fingers and rotate it
Motion 9	Pick up a mobile phone and input the PUK with one hand
Motion 10	Pick up a ping-pong by using chopsticks

The ELONXI SEMG acquisition system adopted in this experiment transmitted the collected SEMG signals to the upper computer for analysis and processing. The system mainly included a main SEMG device, electrode sleeve, universal electrode interface converter, Bluetooth adapter, and electrode connection wire. The sampling electrode was fixed through the electrode sleeve to avoid electrode displacement. The electrode was powered by the universal electrode interface converter, thereby avoiding power frequency interference. The acquisition process of ten kinds of self-designed hand motions is as follows. First, the electrode sleeve was correctly placed on the right forearm and connected with the main SEMG device through the electrode connection. Then the SEMG signals of 6 channels were uploaded to the upper computer via Bluetooth module. The resolution of the system was 16 bits and the sampling frequency was 1024 Hz. The real time SEMG signals were visualised on a computer screen giving participants feedback to choose electrode locations with stronger SEMG signals.

C. SIGNAL PREPROCESSING

SEMG signals are electrical responses caused by the action of muscle fibers during the contraction of multiple muscles. Affected by external environment and acquisition device, the collected original SEMG signals contain lots of noise

signals, such as electrode noise, signal line electromagnetic noise, and broadband noise. Therefore, it is quite important to reduce the noise of original signal to provide real and effective data for feature extraction.

Empirical Mode Decomposition algorithm, firstly proposed by Huang *et al.*, is a data processing method for the self-adaptive decomposition of nonlinear and non-stationary signal [22]. With high time-frequency resolution and good adaptivity, the algorithm, by decomposing the original signal, separates noise from effective signal in different intrinsic mode functions (IMF), so that the reasonable IMF reconstructed signal can be selected. It can not only perfectly reconstruct the original signals, but also effectively remove the noises. Hence, combined with the features of SEMG signal, EMD algorithm is an ideal approach for reducing the noise of SEMG signal.

Algorithm 1 EMD Algorithm for EMG Signal Noise Reduction

Input: The original data series of EMG signal, $X(t), (1, \cdots, 6)$ {t is the acquisition channel };

Output: Intrinsic mode functions, $C_{IMF}(j)$;

1: Repeat
2: **for** all i such as $1 \leq i \leq k$ **do**
3: Find all the extreme points of $X(t)$,namely $P(t) = \{P_{\min}(i), P_{\max}(i)\}$;
4: Fit the extreme points by interpolation method: lower envelope, namely, $P_{\min}(i) \rightarrow E_{\min}(i)$,upper envelope, i.e., $P_{\max}(i) \rightarrow E_{\max}(i)$;
5: Calculate average envelop value,namely, $A(t) = (E_{\min}(i) + E_{\max}(i))/2$;
6: Obtain stationary data series,$S(t) = X(t) - A(t)$;
7: **end for**
8: Obtain the first IMF component,$C_{IMF}(1)$ { repeat steps $3 \sim 6$ on the residual $A(t)$ };
9: Generate new data series $D(1) = X(t) - C_{IMF}(1)$ and repeat steps $3 \sim 8$, then the second IMF component $C_{IMF}(2)$ is obtained;
10: repeat steps $3 \sim 9$ until the last data series $D(n)$ cannot be decomposed, thereby obtaining IMF set, $\{C_{IMF}(1), C_{IMF}(2), \cdots, C_{IMF}(n)\}$

The pseudo code as shown in Algorithm 1, after EMD is performed on each channel's SEMG signal, a set of intrinsic modal functions can be obtained as:

$$\mathbb{C}(t) = \sum_{j}^{n} C_{IMF}(j) + \delta_n \tag{1}$$

Here, δ_n is the residual of original SEMG signal after extracted n IMFs C. The data signal obtained after noise reduction by EMD algorithm ensures the feature extraction of real movement signals.

D. FEATURE EXTRACTION

Lyapunov exponent is the average exponential change rate of adjacent tracks infinitely close in the phase space [23]. It is used to identify the numerical features in dynamic chaotic system and can well represent the sensitivity of the system to the initial value as the variables evolve with time [24]. One N-dimensional system has N Lyapunov exponents, forming an exponential spectrum. When the system dimension L is large, in order to reduce the calculating amount, the predictability of dynamic system is determined by computing the Maximum Lyapunov Exponent (MLE). MLE method is not only an important indicator to distinguish chaotic attractors, but also a quantitative description of sensitivity to initial value. Therefore, it is widely used in machine fault diagnosis as well as muscle contraction and muscle activity detection. Its definition is:

$$\lambda_{\max} = \frac{1}{\Delta t} \sum_{k=1}^{M} \frac{L(t_k)}{L(t_{k-1})} \tag{2}$$

where $L(t_k)$ represents the distance between two nearest zero points at moment t_k, M denotes the total step length, and Δt is the sampling time for obtaining MLE. The distance between adjacent tracks is usually multiplied by the prediction error on the logarithmic scale to obtain the Lyapunov exponent of the whole set of intrinsic modal functions. Its definition is:

$$p(k) = \frac{1}{Nt} \sum_{n=1}^{N} 1b \frac{\Gamma_n(k)}{\Delta n} \tag{3}$$

where N is the total number of phase points, Δn is the distance between phase points X_n and $X_n + 1$ ($X_n + 1$ is the nearest point to X_n), and $\Gamma_n(k)$ is the distance between X_n and $X_n + 1$ after k times of convolution step length. In the $p(k) \backsim k$ diagram, the slope of line is MLE.

In our experiment, the length of overlapping windows is 500 ms, and the increment between windows is 125 ms. The two typical features of SEMG signal, i.e., delay time and embedded dimension, are two very important parameters for calculating Lyapunov exponent. They are suitable for representing the dynamic behavior of SEMG gesture time series data, so they are selected to represent the motion features of SEMG signal.

The delay time was determined by mutual information method, which is defined as:

$$H(\tau) = p(Y_n, Y_{n+\tau}) In \frac{p(Y_n, Y_{n+\tau})}{p(Y_n) p(Y_{n+\tau})} \tag{4}$$

where $p(Y_n)$, $p(Y_{n+\tau})$ and $p(Y_n, Y_{n+\tau})$ are probability values. In the $H(\tau) \backsim \tau$ diagram, τ corresponds to the first local minimum value that appears.

The embedded dimension was calculated by using pseudo neighbor method, which is defined as:

$$E_1(m) = \frac{E(m+1)}{E(m)} \tag{5}$$

where $E(m+1)$ and $E(m)$ are the average thresholds of the distances between all two nearest neighbors in the reconstructed m-dimensional space and $m+1$-dimensional space, respectively. In the $E_1(m) \backsim m$ diagram, when the value of $E_1(m)$ doesn't change significantly with the increase of m,

the smallest embedded dimension value is the $E_1(m)$ to be selected. The MLE eigenvectors obtained by formula (2) and (3) will be used for ten kinds of hand motions recognition by random forest classifier.

E. RANDOM FOREST

Random forest, as a supervised learning algorithm, is a decision tree model based on bagging framework [25]. RF algorithm is widely used in the classification and regression of biomedicine, e-commerce, and human-computer interaction due to its advantages of simple implementation, high precision, strong anti-overfitting ability, and certain anti-noise ability [26]. The RF classifier as shown in Fig.3, is composed of a group of tree classifiers, among which each tress classifier is generated by a random vector samples independently of the input vector sampling. The optimal classification is determined by voting.

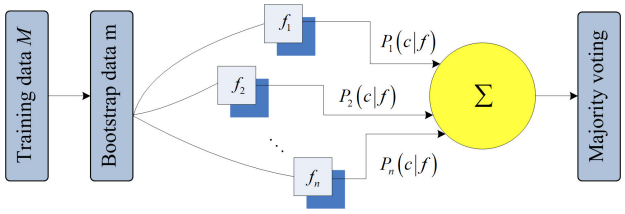

FIGURE 3. Schematic diagram of random forest algorithm.

For a training set M with category K, the probability of randomly selecting a feature and voting it into category k is:

$$p(k) = \sum_{k=1}^{K} p_k (1 - p_k) \tag{6}$$

$$p_k = \sum_{i \neq j} (f(k_i, M)/|M|)\left(f\left(k_j, M\right)/|M|\right) \tag{7}$$

where $f(k_i, M)$ is the probability of the selected feature belonging to category k. Formula (6) is simplified into:

$$p(k) = 1 - \sum_{k=1}^{K} p_k^2 \tag{8}$$

It should be noted that although the training set of each tree is different, these sets contain repeated training samples. Each tree grows as best it can and there is no pruning process. The number of features each node uses to generate the tree and the number of trees to grow are two user-defined parameters needed to generate the random forest classifier.

III. DATA ANALYSIS

In consideration of the nonlinear dynamic signal of SEMG signal, the original SEMG signal was decomposed into a group of IMFs after noise reduction, as shown in Fig.4. It can be seen from Fig.4 that the original SEMG signal $X(t)$ has been decomposed into $C_{IMF}(j), (j = 1, 2, \cdots, 6)$ and deviation δ_n. $C_{IMF}(j)$ is oscillation function with different

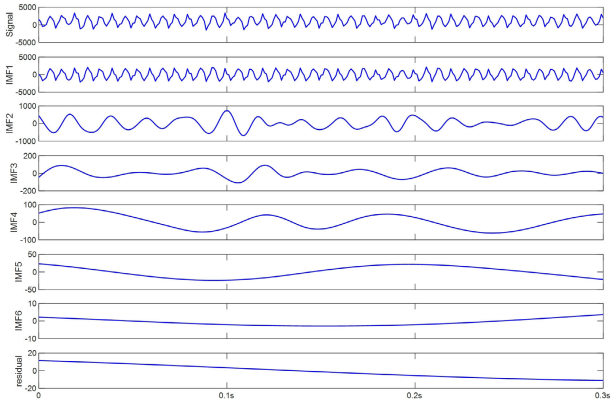

FIGURE 4. EMD decomposition of SEMG signal.

amplitudes and frequencies. δ_n is a monotonic signal, indicating that the drift component obtained by subtracting all $C_{IMF}(j)$ from the original signal $X(t)$ no longer satisfies the decomposition conditions.

Delay time and embedded dimension are two important parameters for calculating Lyapunov exponent. Either the selected delay time is too large or too small is not conducive to the optimization of EMG signal [27]. The delay time τ obtained by mutual information method is shown in Fig.5, where the value of the first local minimum point appears at $\tau = 5$ is used for phase space reconstruction.

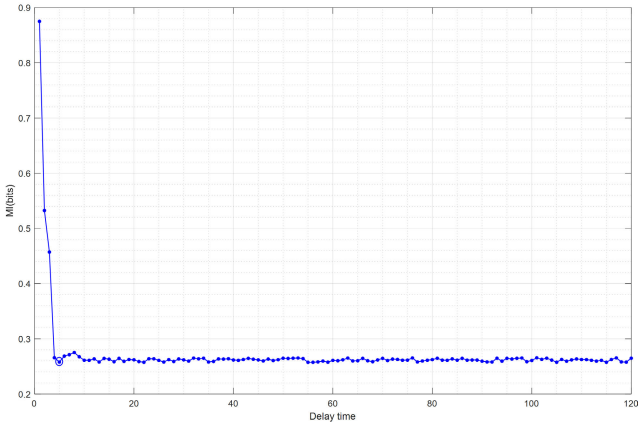

FIGURE 5. Delay time of SEMG signal.

Fig.6 shows the embedded dimension obtained by pseudo-neighbor method. It can be known from the curve that, from $m = 8$, $E_1(m)$ doesn't change significantly with the increase of m and starts to approach to 1 progressively. Hence, the minimum embedded dimension value selected for topology reconstruction in this experiment is 8.

The Lyapunov exponents of SEMG signal are shown in Table 2, whereas the MLEs of SEMG signal calculated through the method mentioned in Section II C and D are presented in Table 3. As shown in Table 2, the ten motions have different mean values (MV) and standard deviations (SD). For the same motion, the mean values and standard

TABLE 2. The LEs of original SEMG signal.

Hand motion	Channel 1 (MV+SD)	Channel 2 (MV+SD)	Channel 3 (MV+SD)	Channel 4 (MV+SD)	Channel 5 (MV+SD)	Channel 6 (MV+SD)
Motion 1	0.1159 ± 0.0147	0.0982 ± 0.0125	0.1754 ± 0.0227	0.1636 ± 0.0214	0.0867 ± 0.0243	0.1584 ± 0.0135
Motion 2	0.1233 ± 0.0176	0.1018 ± 0.0137	0.2091 ± 0.0198	0.1519 ± 0.0187	0.1153 ± 0.0139	0.1942 ± 0.0196
Motion 3	0.1139 ± 0.0124	0.1233 ± 0.0261	0.1649 ± 0.0114	0.1723 ± 0.0172	0.1055 ± 0.0126	0.1841 ± 0.0113
Motion 4	0.1457 ± 0.0211	0.1256 ± 0.0179	0.1883 ± 0.0201	0.1449 ± 0.0157	0.1069 ± 0.0110	0.2040 ± 0.0229
Motion 5	0.1253 ± 0.0249	0.1141 ± 0.0118	0.2037 ± 0.0195	0.1452 ± 0.0119	0.0935 ± 0.0117	0.1995 ± 0.0264
Motion 6	0.1146 ± 0.0133	0.1327 ± 0.0154	0.1871 ± 0.0154	0.1693 ± 0.0120	0.1010 ± 0.0174	0.2271 ± 0.0177
Motion 7	0.1662 ± 0.0211	0.1097 ± 0.0113	0.1993 ± 0.0226	0.1834 ± 0.0258	0.1295 ± 0.0187	0.1743 ± 0.0134
Motion 8	0.1571 ± 0.0185	0.1389 ± 0.0175	0.1769 ± 0.0189	0.1970 ± 0.0167	0.1633 ± 0.0331	0.2359 ± 0.0341
Motion 9	0.1820 ± 0.0171	0.1176 ± 0.0191	0.1735 ± 0.0177	0.1694 ± 0.0162	0.1227 ± 0.0190	0.1984 ± 0.0165
Motion 10	0.1368 ± 0.0169	0.1154 ± 0.0142	0.2113 ± 0.0243	0.1876 ± 0.0218	0.1264 ± 0.0114	0.1938 ± 0.0221

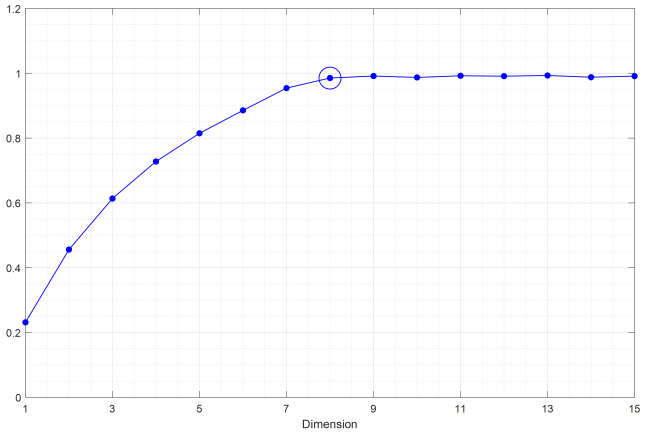

FIGURE 6. Embedded dimension of SEMG signal.

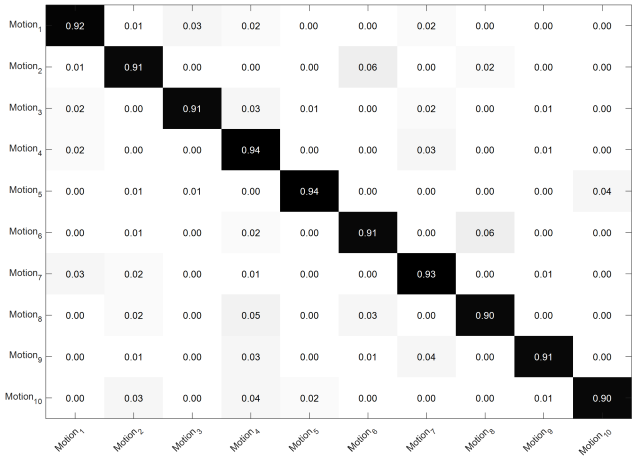

FIGURE 7. Hybrid matrix of recognition rates of ten in-hand motions.

deviations of different channels are different. Compared with other channels, the values of Channel 2 are small and fluctuate in a small range. It should be noted that, low Lyapunov exponent is crucial to improving the recognition accuracy of RF classifier.

The MLEs of the decomposition IMFs shown in Table 3 illustrate the detailed IMFs information based on different channels. Notice that the MV and SD of LEs are slightly higher for the original signals, whereas the MV and SD of MLEs are lower after decomposition. the eigenvalues of IMFs $C_{IMF}(j)$ $(j = 1, \cdots, 6)$ were selected as features for MLE. Overall, the MLEs of the collected SEMG signal is suitable for feature extraction and can provide appropriate training samples for RF classifier.

IV. EXPERIMENTAL RESULTS

A. MOTION RECOGNITION BASED ON RANDOM FOREST

To verify the identification performance of the hand motion recognition system, the recognition rates of ten hand motions obtained by random forest classifier are shown in Fig.7. The average recognition rate of the ten motions is 91.67%. The values in black rectangles in Fig.7 are the average motion recognition rates; the others are the rates of deviation between two motions. Generally speaking, the recognition rates of the motions have excessed 90%, except for Motions 8 and 10, whose recognition rates are only 90%. Moreover, the recognition rates of Motions 4 and 5 are the highest, reaching 94%, reflecting the good classification performance of the system. Although the recognition rates of Motions 2 and 6 have reached 91%, the rate of deviation between them is as high as 6%, which is the same as that between Motions 6 and 8. By contrast, the rates of deviation between other motions range from 1% to 5%.

B. COMPARISON OF MOTION RECOGNITION RATES BASED ON DIFFERENT SUBJECTS

As the object operation habits and grasping manner of subjects differ, they can grasp one object stably by the same movement yet different operation ways. Though the subjects had undergone rigorous training on grasping manner, grasping point, and number of fingers used before the experiment, there were still individual differences in the myoelectric activity information of hand motions. Hence, it is necessary to investigate the influences caused by the individual differences of different subjects on the recognition results of the same motion. Fig.8 indicates the box plot of different in-hand motion recognition results for the different subjects.

As shown in Fig.8, the average motion recognition rates of the subjects differ significantly. Specifically, the average recognition rate of Subject 5 is the lowest, only 89.12%; and the average recognition rate of Subject 6 is the highest, reaching 94.23%. Besides, the recognition rates of

TABLE 3. The MLEs of the decomposition IMFs.

Hand motion	IMFs	Channel 1 (MV+SD)	Channel 2 (MV+SD)	Channel 3 (MV+SD)	Channel 4 (MV+SD)	Channel 5 (MV+SD)	Channel 6 (MV+SD)
Motion 1	IMF 1	0.1352 ± 0.0163	0.1145 ± 0.0157	0.2057 ± 0.0358	0.1937 ± 0.0326	0.1152 ± 0.0342	0.1895 ± 0.0234
	IMF 2	0.1223 ± 0.0269	0.1033 ± 0.0248	0.1836 ± 0.0129	0.1864 ± 0.0277	0.1095 ± 0.0241	0.1776 ± 0.0257
	IMF 3	0.1178 ± 0.0314	0.0972 ± 0.0151	0.1729 ± 0.0136	0.1749 ± 0.0134	0.1012 ± 0.0176	0.1662 ± 0.0138
	IMF 4	0.1127 ± 0.0135	0.0849 ± 0.0205	0.1662 ± 0.0122	0.1628 ± 0.3271	0.0956 ± 0.0128	0.1559 ± 0.0153
	IMF 5	0.1074 ± 0.0286	0.0793 ± 0.0117	0.1597 ± 0.0136	0.1579 ± 0.0118	0.0876 ± 0.0233	0.1492 ± 0.0241
	IMF 6	0.0932 ± 0.0128	0.0721 ± 0.0176	0.1512 ± 0.0203	0.1457 ± 0.0226	0.0758 ± 0.0267	0.1337 ± 0.0167
Motion 2	IMF 1	0.1573 ± 0.0225	0.1251 ± 0.0267	0.2438 ± 0.0237	0.1623 ± 0.0139	0.1352 ± 0.0168	0.2134 ± 0.0292
	IMF 2	0.1492 ± 0.0217	0.1178 ± 0.0210	0.2356 ± 0.0214	0.1572 ± 0.0234	0.1267 ± 0.0267	0.2037 ± 0.0167
	IMF 3	0.1347 ± 0.0156	0.1092 ± 0.0126	0.2279 ± 0.0164	0.1496 ± 0.0177	0.1169 ± 0.0148	0.1966 ± 0.0179
	IMF 4	0.1219 ± 0.0203	0.0976 ± 0.0138	0.2138 ± 0.0195	0.1358 ± 0.0231	0.1063 ± 0.0273	0.1838 ± 0.0261
	IMF 5	0.1174 ± 0.0155	0.0912 ± 0.0095	0.1978 ± 0.0236	0.1294 ± 0.0132	0.0953 ± 0.0164	0.1793 ± 0.0121
	IMF 6	0.1026 ± 0.0278	0.0856 ± 0.0136	0.1893 ± 0.0168	0.1146 ± 0.0264	0.0876 ± 0.0135	0.1625 ± 0.0114
Motion 3	IMF 1	0.1322 ± 0.0297	0.1357 ± 0.0168	0.1975 ± 0.0342	0.1962 ± 0.0167	0.1242 ± 0.0134	0.1927 ± 0.0231
	IMF 2	0.1265 ± 0.0138	0.1295 ± 0.0193	0.1846 ± 0.0237	0.1853 ± 0.0244	0.1193 ± 0.0267	0.1876 ± 0.0165
	IMF 3	0.1194 ± 0.0117	0.1176 ± 0.0264	0.1763 ± 0.0118	0.1769 ± 0.0116	0.1025 ± 0.0111	0.1778 ± 0.0124
	IMF 4	0.1032 ± 0.0124	0.1092 ± 0.0114	0.1695 ± 0.0123	0.1646 ± 0.0162	0.0978 ± 0.0235	0.1669 ± 0.0231
	IMF 5	0.0983 ± 0.0177	0.0986 ± 0.0167	0.1553 ± 0.0149	0.1521 ± 0.0138	0.0885 ± 0.0192	0.1593 ± 0.0167
	IMF 6	0.0819 ± 0.0237	0.0895 ± 0.0251	0.1442 ± 0.0168	0.1447 ± 0.0166	0.0768 ± 0.0174	0.1501 ± 0.0121
Motion 4	IMF 1	0.1782 ± 0.0237	0.1367 ± 0.0175	0.2026 ± 0.0237	0.1662 ± 0.0114	0.1234 ± 0.0162	0.2342 ± 0.0322
	IMF 2	0.1657 ± 0.0262	0.1296 ± 0.0261	0.1985 ± 0.0167	0.1553 ± 0.0167	0.1168 ± 0.0164	0.2216 ± 0.0227
	IMF 3	0.1579 ± 0.0146	0.1234 ± 0.0112	0.1886 ± 0.0134	0.1467 ± 0.0234	0.1074 ± 0.0237	0.2165 ± 0.0174
	IMF 4	0.1495 ± 0.0231	0.1176 ± 0.0193	0.1779 ± 0.0135	0.1395 ± 0.0175	0.0986 ± 0.0186	0.2056 ± 0.0292
	IMF 5	0.1411 ± 0.0217	0.1085 ± 0.0264	0.1695 ± 0.0233	0.1301 ± 0.0282	0.0875 ± 0.0242	0.1986 ± 0.0134
	IMF 6	0.1326 ± 0.0175	0.0986 ± 0.0137	0.1557 ± 0.0146	0.1225 ± 0.0136	0.0795 ± 0.0166	0.1878 ± 0.0256
Motion 5	IMF 1	0.1467 ± 0.0247	0.1229 ± 0.0187	0.2235 ± 0.0221	0.1677 ± 0.0267	0.1164 ± 0.0266	0.2138 ± 0.0277
	IMF 2	0.1382 ± 0.0236	0.1185 ± 0.0135	0.2186 ± 0.0175	0.1596 ± 0.0181	0.1067 ± 0.0142	0.2064 ± 0.0271
	IMF 3	0.1296 ± 0.0172	0.1079 ± 0.0205	0.2074 ± 0.0234	0.1445 ± 0.0264	0.0987 ± 0.0221	0.1943 ± 0.0182
	IMF 4	0.1223 ± 0.0165	0.0964 ± 0.0172	0.1988 ± 0.0147	0.1396 ± 0.0175	0.0902 ± 0.0150	0.1856 ± 0.0179
	IMF 5	0.1184 ± 0.0297	0.0897 ± 0.0142	0.1872 ± 0.0267	0.1276 ± 0.0267	0.0826 ± 0.0114	0.1723 ± 0.0266
	IMF 6	0.1055 ± 0.0214	0.0822 ± 0.0121	0.1795 ± 0.0164	0.1143 ± 0.0217	0.0762 ± 0.0162	0.1621 ± 0.0176
Motion 6	IMF 1	0.1321 ± 0.0164	0.1526 ± 0.0213	0.2044 ± 0.0134	0.1875 ± 0.0163	0.1232 ± 0.0197	0.2461 ± 0.0212
	IMF 2	0.1267 ± 0.0178	0.1437 ± 0.0171	0.1945 ± 0.0261	0.1774 ± 0.0137	0.1164 ± 0.0113	0.2346 ± 0.0231
	IMF 3	0.1196 ± 0.0131	0.1358 ± 0.0134	0.1875 ± 0.0164	0.1638 ± 0.0167	0.1018 ± 0.0261	0.2266 ± 0.0174
	IMF 4	0.1132 ± 0.0110	0.1273 ± 0.0168	0.1694 ± 0.0267	0.1593 ± 0.0143	0.0942 ± 0.0192	0.2135 ± 0.0141
	IMF 5	0.1026 ± 0.0174	0.1146 ± 0.0194	0.1576 ± 0.0138	0.1464 ± 0.0134	0.0872 ± 0.0135	0.2058 ± 0.0178
	IMF 6	0.0935 ± 0.0126	0.1023 ± 0.0224	0.1479 ± 0.0168	0.1395 ± 0.0103	0.0794 ± 0.0111	0.1877 ± 0.0235
Motion 7	IMF 1	0.1877 ± 0.0214	0.1157 ± 0.0112	0.2231 ± 0.0243	0.1876 ± 0.0254	0.1417 ± 0.0182	0.1975 ± 0.0164
	IMF 2	0.1775 ± 0.0163	0.1074 ± 0.0178	0.2164 ± 0.0314	0.1795 ± 0.0214	0.1392 ± 0.0217	0.1876 ± 0.0192
	IMF 3	0.1689 ± 0.0187	0.0981 ± 0.0126	0.2077 ± 0.0175	0.1683 ± 0.0346	0.1258 ± 0.0234	0.1766 ± 0.0179
	IMF 4	0.1534 ± 0.0172	0.0925 ± 0.0114	0.1982 ± 0.0168	0.1597 ± 0.0261	0.1167 ± 0.0167	0.1712 ± 0.0978
	IMF 5	0.1421 ± 0.0138	0.0876 ± 0.0135	0.1879 ± 0.0194	0.1456 ± 0.0278	0.1053 ± 0.0191	0.1645 ± 0.0167
	IMF 6	0.1392 ± 0.0972	0.0764 ± 0.0172	0.1772 ± 0.0237	0.1392 ± 0.0241	0.0946 ± 0.0178	0.1532 ± 0.0131
Motion 8	IMF 1	0.1642 ± 0.0213	0.1446 ± 0.0162	0.1944 ± 0.0188	0.2001 ± 0.0178	0.1867 ± 0.0241	0.2451 ± 0.0312
	IMF 2	0.1574 ± 0.0167	0.1395 ± 0.0135	0.1872 ± 0.0166	0.1857 ± 0.0142	0.1712 ± 0.0137	0.2278 ± 0.0274
	IMF 3	0.1493 ± 0.0210	0.1268 ± 0.0143	0.1735 ± 0.0197	0.1753 ± 0.0173	0.1518 ± 0.0412	0.2143 ± 0.0281
	IMF 4	0.1375 ± 0.0189	0.1186 ± 0.0107	0.1642 ± 0.0135	0.1620 ± 0.0107	0.1428 ± 0.0267	0.1975 ± 0.0216
	IMF 5	0.1268 ± 0.0173	0.1094 ± 0.1324	0.1521 ± 0.0172	0.1527 ± 0.0186	0.1310 ± 0.0172	0.1815 ± 0.0172
	IMF 6	0.1169 ± 0.0187	0.0975 ± 0.0157	0.1462 ± 0.0172	0.1412 ± 0.1324	0.1198 ± 0.0224	0.1726 ± 0.0147
Motion 9	IMF 1	0.2017 ± 0.0213	0.1279 ± 0.0167	0.1921 ± 0.0220	0.1772 ± 0.0126	0.1378 ± 0.0172	0.2103 ± 0.0156
	IMF 2	0.1876 ± 0.0234	0.1147 ± 0.0134	0.1812 ± 0.0164	0.1641 ± 0.0174	0.1224 ± 0.0170	0.2012 ± 0.0175
	IMF 3	0.1779 ± 0.0167	0.1082 ± 0.0121	0.1698 ± 0.0143	0.1592 ± 0.0146	0.1181 ± 0.0921	0.1875 ± 0.0125
	IMF 4	0.1689 ± 0.0131	0.0975 ± 0.0172	0.1578 ± 0.0166	0.1477 ± 0.0168	0.1012 ± 0.0124	0.1785 ± 0.0172
	IMF 5	0.1546 ± 0.0192	0.0876 ± 0.0164	0.1479 ± 0.0130	0.1390 ± 0.0172	0.0952 ± 0.0141	0.1624 ± 0.0110
	IMF 6	0.1462 ± 0.0173	0.0795 ± 0.0187	0.1323 ± 0.0178	0.1274 ± 0.0166	0.0864 ± 0.0109	0.1521 ± 0.0137
Motion 10	IMF 1	0.1425 ± 0.0162	0.1264 ± 0.0126	0.2234 ± 0.0231	0.1895 ± 0.0127	0.1426 ± 0.0164	0.2031 ± 0.0231
	IMF 2	0.1376 ± 0.0121	0.1175 ± 0.0098	0.2061 ± 0.0167	0.1723 ± 0.0181	0.1375 ± 0.0098	0.1879 ± 0.0167
	IMF 3	0.1292 ± 0.0178	0.1023 ± 0.0114	0.1925 ± 0.0194	0.1645 ± 0.0129	0.1241 ± 0.0113	0.1752 ± 0.0182
	IMF 4	0.1164 ± 0.0214	0.0902 ± 0.0178	0.1876 ± 0.0182	0.1541 ± 0.0142	0.1112 ± 0.0162	0.1642 ± 0.0138
	IMF 5	0.1016 ± 0.0127	0.0756 ± 0.0125	0.1764 ± 0.0164	0.1410 ± 0.0131	0.1043 ± 0.0172	0.1501 ± 0.0143
	IMF 6	0.0931 ± 0.0116	0.0647 ± 0.0131	0.1647 ± 0.0192	0.1295 ± 0.0167	0.0920 ± 0.0141	0.1426 ± 0.0184

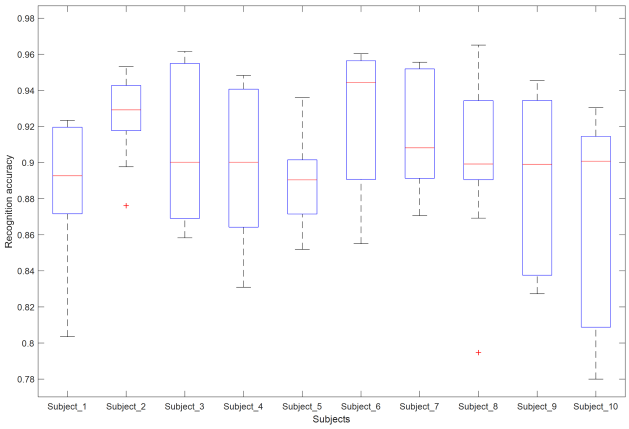

FIGURE 8. Recognition rates with different subjects.

Subjects 2 and 8 fluctuate wildly, and the corresponding maximum rates of deviation reach 12.67% and 20.45%, respectively. The main reason for this result is probably the non-standard manipulation of some motions. Hence, the influence of different subjects on the final experimental results can not be ignored. In general, the recognition rates of most subjects are above 90%. The results in Fig.8 show that individual differences have certain influence on the analysis of SEMG signal.

C. DIFFERENT MACHINE LEARNING ALGORITHMS BASED RECOGNITION

To verify the effect of complex in-hand motion recognition based on RF algorithm, the results of this experiment were compared with those obtained through three conventional machine learning algorithms, namely, Support Vector Machine (SVM), Neural Network (NN) and k-Nearest Neighbor (KNN). SVM method is a supervised machine learning algorithm which realizes binary classification by finding the hyperplane of data samples and obtaining the maximum margin. NN method is a machine learning algorithm that realizes the classification of data samples by simulating the behavior characteristics of human brain neural network and adjusting the weight of the interconnection between nodes of hidden layer. As one of the simplest machine learning algorithms, the principle of KNN classifier is that if most of the k most similar samples in the feature space belong to a category, then the sample also belongs to this category. These three classification algorithms have been widely used in such fields as information processing and pattern recognition.

Before the experiment, the kernel function and parameters corresponding to SVM classifier and NN classifier should be selected to ensure their classification performances. Gaussian kernel function is used as the kernel function of support vector machine. The values of penalty parameter C and nuclear radius γ are shown in $(C, \gamma) = (1, 0.0216)$. Identity activation function is used in neural network. The number of nodes of input layer I, the number of nodes of hidden layer H, and the number of nodes of output layer O are shown in $(I, H, O) = (2, 7, 10)$. The number of nearest neighbors, $k = 5$, is determined for KNN classifier.

TABLE 4. Classification rates with different classifiers.

Hand motion	Classifier	Everage recognition rate ± SD
Motion 1	RF	92.05% ± 0.24
	SVM	92.03% ± 0.31
	NN	91.33% ± 0.61
	KNN	90.82% ± 0.43
Motion 2	RF	91.27% ± 0.27
	SVM	91.05% ± 0.54
	NN	88.55% ± 1.12
	KNN	89.08% ± 0.67
Motion 3	RF	90.89% ± 0.47
	SVM	89.75% ± 0.28
	NN	89.34% ± 0.67
	KNN	88.53% ± 0.53
Motion 4	RF	94.24% ± 0.84
	SVM	92.14% ± 0.69
	NN	93.28% ± 1.15
	KNN	91.32% ± 0.95
Motion 5	RF	93.86% ± 0.45
	SVM	91.17% ± 0.50
	NN	89.56% ± 0.51
	KNN	88.51% ± 0.33
Motion 6	RF	91.28% ± 0.47
	SVM	90.53% ± 0.50
	NN	86.02% ± 0.70
	KNN	88.07% ± 0.64
Motion 7	RF	93.02% ± 0.37
	SVM	93.32% ± 0.65
	NN	90.29% ± 0.71
	KNN	90.05% ± 1.03
Motion 8	RF	90.15% ± 0.15
	SVM	91.23% ± 0.31
	NN	89.08% ± 0.69
	KNN	89.45% ± 0.90
Motion 9	RF	91.41% ± 0.23
	SVM	90.47% ± 0.34
	NN	86.64% ± 0.42
	KNN	88.50% ± 0.30
Motion 10	RF	89.75% ± 0.16
	SVM	87.23% ± 0.22
	NN	86.93% ± 0.48
	KNN	85.61% ± 0.58

Table 4 and Fig.9 show the human in-hand motion recognition results obtained by four machine learning algorithms. The average recognition rates based on SVM, NN and KNN are 90.89%, 89.1% and 88.99%, respectively, which are lower than that based on RF classifier (91.67%). From table 4 it can be seen that the SD values of recognition rates based on SVM, NN and KNN are higher for the RF method. Overall, in terms of different methods and subjects, RF classifier always presents the best performance.

As can be known from Fig.9, RF and SVM algorithms have similar recognition rates for Motion 1 and Motion 7. Specifically, SVM algorithm has the highest recognition rates

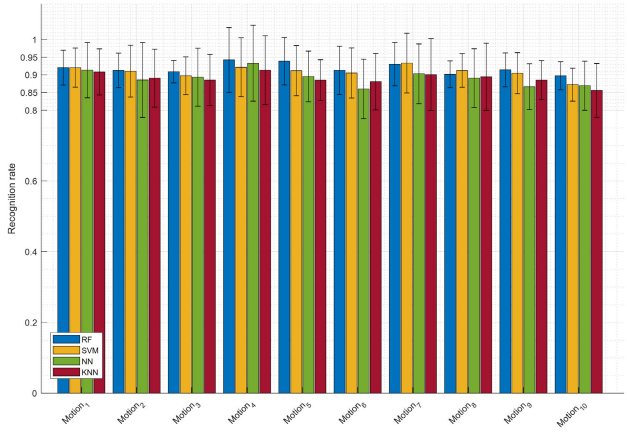

FIGURE 9. The comparison of four methods.

for Motions 7 and 8, while NN algorithm has the lowest recognition rates for Motions 2, 6, 8 and 9. For Motion 10, the recognition rate based on KNN classifier is lowest, only 85.61%. The standard deviation reflects the fluctuation of recognition rate of the same hand motion by different algorithms. The fluctuation range of Motions 4, 6 and 7 based on four algorithms are wider and those based on RF and SVM algorithms are smaller. On the whole, the hand motion recognition accuracies of RF are superior to those of the other three algorithms, reflecting the good classification performance RF algorithm.

V. CONCLUSION

An SEMG-based human in-hand motion recognition system is proposed in this paper by using nonlinear time series analysis methods. The system is composed of five parts, namely, human upper limb determination, data collection, data preprocessing, feature extraction, and recognition algorithm, and is illustrated in detail from human upper limb determination, data acquisition and process, and motion recognition. For data acquisition and processing, nonlinear time series analysis methods, including EMD and MLE, are adopted to process SEMG signals and obtain real and effective motion features. For the motion recognition, RF algorithm is used for hand movement recognition and to analyze the influence of different subjects on recognition rates. From the data analysis, the nonlinear time series method is proved to be a good substitute for SEMG signal processing. RF algorithm, whose recognition rate is 91.67%, is compared with SVM, NN and KNN algorithms to verify its superiority. Because of the complex properties involved in the human hand motions, a single sensor can get a certain feature information for some motion recognition. Although experimental results illustrate that the human in-hand motion recognition system proposed in this paper can effectively recognize these different in-hand movements with a better performance than other popular methods, further research would be focused on improving human in-hand motion recognition efficiency based on multiple sensors for real-time applications in human-robot interaction and bionic prosthetic hand control.

REFERENCES

[1] Y. Xue, Z. Ju, K. Xiang, J. Chen, and H. Liu, "Multimodal human hand motion sensing and analysis—A review," *IEEE Trans. Cogn. Devel. Syst.*, vol. 11, no. 2, pp. 162–175, Jun. 2019.
[2] M. Z. Poh, N. C. Swenson, and R. W. Picard, "A wearable sensor for unobtrusive, long-term assessment of electrodermal activity," *IEEE Trans. Biomed. Eng.*, vol. 57, no. 5, pp. 1243–1252, May 2010.
[3] Z. Ju and H. Liu, "Human hand motion analysis with multisensory information," *IEEE/ASME Trans. Mechatronics*, vol. 19, no. 2, pp. 456–466, Apr. 2014.
[4] F. Duan and L. L. Dai, "Recognizing the gradual changes in sEMG characteristics based on incremental learning of wavelet neural network ensemble," *IEEE Trans. Ind. Electron.*, vol. 64, no. 5, pp. 4276–4286, May 2017.
[5] W. Guo, X. Sheng, H. Liu, and X. Zhu, "Development of a multi-channel compact-size wireless hybrid SEMG/NIRS sensor system for prosthetic manipulation," *IEEE Sensors J.*, vol. 16, no. 2, pp. 447–456, Jan. 2016.
[6] Y. Xue, Z. Ju, K. Xiang, J. Chen, and H. Liu, "Multiple sensors based hand motion recognition using adaptive directed acyclic graph," *Appl. Sci.*, vol. 7, no. 4, p. 358, 2017.
[7] J.-S. Wang and F.-C. Chuang, "An accelerometer-based digital pen with a trajectory recognition algorithm for handwritten digit and gesture recognition," *IEEE Trans. Ind. Electron.*, vol. 59, no. 7, pp. 2998–3007, Jul. 2012.
[8] J. S. Wang and F. C. Chuang, "Towards robot-assisted post-stroke hand rehabilitation: Fugl-Meyer gesture recognition using sEMG," in *Proc. CYBER*, Honolulu, HI, USA, 2018, pp. 1472–1477.
[9] U. Cote-Allard, C. L. Fall, A. Campeau-Lecours, C. Gosselin, F. Laviolette, and B. Gosselin, "Transfer learning for sEMG hand gestures recognition using convolutional neural networks," in *Proc. SMC*, Banff, AB, Canada, 2017, pp. 1663–1668.
[10] S. Lobov, V. Mironov, V. Kazantsev, and I. Kastalskiy, "A spiking neural network in sEMG feature extraction," *Sensors*, vol. 15, no. 11, pp. 27894–27904, Nov. 2015.
[11] S. M. Mane, R. A. Kambli, F. S. Kazi, and N. M. Singh, "Hand motion recognition from single channel surface EMG using wavelet & artificial neural network," *Procedia Comput. Sci.*, vol. 49, pp. 58–65, Nov. 2015.
[12] G. D. Fraser, A. D. C. Chan, J. R. Green, and D. T. Macisaac, "Automated biosignal quality analysis for electromyography using a one-class support vector machine," *IEEE Trans. Instrum. Meas.*, vol. 63, no. 12, pp. 2919–2930, Dec. 2014.
[13] X. Hu, J. Kan, and W. Li, "Classification of surface electromyogram signals based on directed acyclic graphs and support vector machines," *Turkish J. Electr. Eng. Comput. Sci.*, vol. 26, no. 2, pp. 732–742, Mar. 2018.
[14] W. Wei, Y. Hu, and Y. Du, "A Comprehensive evaluation of support vector machine in hand movement classification using surface electromyography," *Nanosci. Nanotechnol. Lett.*, vol. 9, no. 5, pp. 741–753, May 2017.
[15] Y. S. Razin, K. Pluckter, J. Ueda, and K. Feigh, "Predicting task intent from surface electromyography using layered hidden Markov models," *IEEE Robot. Autom. Lett.*, vol. 2, no. 2, pp. 1180–1185, Apr. 2017.
[16] N. Malešević, D. Marković, G. Kanitz, M. Controzzi, C. Cipriani, and C. Antfolk, "Vector autoregressive hierarchical hidden Markov models for extracting finger movements using multichannel surface EMG signals," *Complexity*, vol. 2018, pp. 1–12, Feb. 2018.
[17] S. Park, D. Lee, W. K. Chung, and K. Kim, "Hierarchical motion segmentation through sEMG for continuous lower limb motions," *IEEE Robot. Autom. Lett.*, vol. 4, no. 4, pp. 4402–4409, Oct. 2019.
[18] J. Ben Ali, N. Fnaiech, L. Saidi, B. Chebel-Morello, and F. Fnaiech, "Application of empirical mode decomposition and artificial neural network for automatic bearing fault diagnosis based on vibration signals," *Appl. Acoust.*, vol. 89, no. 3, pp. 16–27, Mar. 2015.
[19] J. Pathak, Z. Lu, B. R. Hunt, M. Girvan, and E. Ott, "Using machine learning to replicate chaotic attractors and calculate Lyapunov exponents from data," *Chaos, Interdiscipl. J. Nonlinear Sci.*, vol. 118, no. 8, Feb. 2017, Art. no. 121102.
[20] Q. Ai, Q. Liu, T. Yuan, and Y. Lu, "Gestures recognition based on wavelet and LLE," *Australas. Phys. Eng. Sci. Med.*, vol. 36, no. 2, pp. 167–176, Jun. 2013.
[21] Y. Guo, G. R. Naik, S. Huang, A. Abraham, and H. T. Nguyen, "Nonlinear multiscale Maximal Lyapunov Exponent for accurate myoelectric signal classification," *Appl. Soft Comput.*, vol. 36, pp. 633–640, Nov. 2015.

[22] N. E. Huang, Z. Shen, S. R. Long, M. C. Wu, H. H. Shih, Q. Zheng, N.-C. Yen, C. C. Tung, and H. H. Liu, "The empirical mode decomposition and the Hilbert spectrum for nonlinear and non-stationary time series analysis," *Proc. Roy. Soc. London Ser. A, Math., Phys. Eng. Sci.*, vol. 454, no. 1971, pp. 903–995, Mar. 1998.
[23] M. T. Rosenstein, J. J. Collins, and C. J. De Luca, "A practical method for calculating largest Lyapunov exponents from small data sets," *Phys. D, Nonlinear Phenomena*, vol. 65, no. 2, pp. 117–137, May 1993.
[24] S. Kwon, Y. Kim, and J. Kim, "Movement stability analysis of surface electromyography-based elbow power assistance," *IEEE Trans. Biomed. Eng.*, vol. 61, no. 4, pp. 1134–1142, Apr. 2014.
[25] L. Breiman, "Random forests," *Mach. Learn.*, vol. 45, no. 1, pp. 5–32, Oct. 2001.
[26] A. Verikas, A. Gelzinis, and M. Bacauskiene, "Mining data with random forests: A survey and results of new tests," *Pattern Recognit.*, vol. 44, no. 2, pp. 330–349, Feb. 2011.
[27] Z. Ju, G. Ouyang, M. Wilamowska-Korsak, and H. Liu, "Surface EMG based hand manipulation identification via nonlinear feature extraction and classification," *IEEE Sensors J.*, vol. 13, no. 9, pp. 3302–3311, Sep. 2013.

YAXU XUE received the B.S. degree in electronic information engineering from Xinyang Normal University, Xinyang, China, the M.S. degree in control science and engineering from Chongqing University, Chongqing, China, in 2011, and the Ph.D. degree from the Traffic Information Engineering and Control, Wuhan University of Technology, Wuhan, China. He is currently a Lecturer with the School of Electrical and Mechanical Engineering, Pingdingshan University, Pingdingshan, China. His research interests are hand motion signal analysis and machine learning.

XIAOFEI JI received the M.S. and Ph.D. degrees from Liaoning Shihua University and the University of Portsmouth, in 2003 and 2010, respectively.

From 2003 to 2012, she was a Lecturer with the School of Automation, Shenyang Aerospace University. Since 2013, she has been holding a position as an Associate Professor with Shenyang Aerospace University. She has published over 40 technical research articles and one book. More than 20 research articles have been indexed by SCI/EI. Her research interests include vision analysis and pattern recognition. She is the leader of National Natural Science Fund Project and main group member of Six National and Local Government Projects.

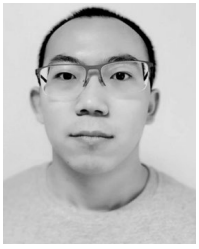

DALIN ZHOU received the B.S. degree in automation from the University of Science and Technology of China, Hefei, China, in 2012, and the Ph.D. degree in computing from the University of Portsmouth, U.K., in 2018. He is currently a Lecturer in computer science with the Intelligent System and Biomedical Robotics Group, University of Portsmouth, Portsmouth, U.K. His research interests include bio-signal processing, machine learning, human behavior analysis, human–machine interface, and assistive technology for rehabilitation.

JING LI received the B.E. degree in electronic information engineering from Nanchang University, China, in 2005, and the Ph.D. degree in electronic and electrical engineering from the University of Sheffield, U.K., in 2011. From 2011 to 2012, she was a Research Associate with the Department of Computer Science, University of Sheffield. She is currently an Associate Professor with the School of Information Engineering, Nanchang University. She has authored or coauthored in various journals, such as the IEEE TRANSACTIONS ON INDUSTRIAL INFORMATICS, the IEEE TRANSACTIONS ON IMAGE PROCESSING, and *Information Sciences* (Elsevier). Her research interests include content-based image retrieval, visual tracking, behavior recognition, and scene understanding in complex environments.

ZHAOJIE JU (M'08–SM'16) received the B.S. degree in automatic control and the M.S. degree in intelligent robotics from the Huazhong University of Science and Technology, China, and the Ph.D. degree in intelligent robotics from the University of Portsmouth, U.K.

He held a Research appointment at University College London, London, U.K., before he started his independent academic position at the University of Portsmouth, U.K., in 2012. He is currently a Reader in machine learning and robotics with the University of Portsmouth, U.K. He has authored or coauthored over 180 publications in journals, book chapters, and conference proceedings. His research interests include machine intelligence, pattern recognition, and their applications on human motion analysis, multifingered robotic hand control, human–robot interaction and collaboration, and robot skill learning.

Dr. Ju received four best paper awards and one Best AE Award in ICRA2018. He is an Associate Editor of the IEEE TRANSACTIONS ON CYBERNETICS, the *Journal of Intelligent and Fuzzy Systems*, the *International Journal of Fuzzy Systems*, and the *Chinese Journal of Mechanical Engineering*.